Structured Multi-Antenna Grassmannian Constellations for Noncoherent Communications

Diego Cuevas[1], Carlos Beltrán[2], Mikel Gutiérrez[1], Ignacio Santamaria[1] and Vít Tuček[3]

[1]Dept. of Communications Engineering, Universidad de Cantabria, Spain
[2]Dept. of Mathematics, Statistics and Computing, Universidad de Cantabria, Spain
[3]Dept. of Wireless Algorithms, Huawei Technologies, Sweden

***Abstract*—In this paper, we propose a new structured Grassmannian constellation for noncoherent communications over multiple-input multiple-output (MIMO) Rayleigh block-fading channels with two transmit antennas. The constellation, which we call Grass-Lattice, is based on a measure preserving mapping from the unit hypercube to the Grassmann manifold. The constellation structure allows for on-the-fly symbol generation and low-complexity decoding. Simulation results show that Grass-Lattice offers a superior bit error rate performance than other structured Grassmannian constellations such as Exp-Map.**

***Index Terms*—Noncoherent communications, Grassmannian constellations, MIMO channels, measure-preserving mapping.**

I. Introduction

In communications over fading channels, the channel state information (CSI) is typically estimated at the receiver side by sending a few known pilots and then used for decoding at the receiver and/or for precoding at the transmitter. These are known as coherent schemes. However, in scenarios dominated by fast fading or massive MIMO systems dedicated to ultra-reliable low-latency communications (URLLC), getting an accurate channel estimate would require pilots to occupy a disproportionate fraction of communication resources. The advent of 5G and beyond (B5G) systems has introduced these novel scenarios that underscore the need for noncoherent communications schemes in which neither the transmitter nor the receiver has any knowledge about the instantaneous CSI.

Despite the absence of CSI at the receiver, noncoherent communication schemes can achieve a substantial fraction of the coherent capacity when the signal-to-noise ratio (SNR) is high, as shown in [1]–[4]. These works proved that at high SNR in the presence of additive Gaussian noise, and assuming a Rayleigh block-fading MIMO channel with coherence time $T \geq 2M$ symbol periods (where M denotes the number of transmit antennas), the optimal strategy for attaining capacity is to transmit isotropically distributed unitary matrices belonging to the Grassmann manifold.

Significant research efforts have been dedicated to the design of noncoherent constellations as optimal packings on the Grassmann manifold [5]–[18]. These constellation designs generally fall into two overarching categories: structured and unstructured. Within the realm of unstructured designs, we can mention the alternating projection method [6], the numerical methods in [7]–[10], which optimize certain distance measures on the Grassmannian (e.g., chordal or spectral), and the methods outlined in [11] and [12], which aim to maximize the diversity product [19].

On the other side, structured designs impose some kind of structure on the constellation points, facilitating low-complexity constellation mapping and demapping. These designs use algebraic constructions, such as the Fourier-based constellation in [13], the uniquely factorable constellations in [20] or the analog subspace codes proposed in [14], group representations [15], [16], parameterized mappings of unitary matrices, such as the Exp-Map design in [17], or structured partitions of the Grassmannian like the Cube-Split constellation [18]. The main disadvantage of these methods is that most of them can only be used in scenarios with single-antenna transmitters. Therefore, we propose an extension of the Grass-Lattice method, which was proposed in [21], [22], to the case $M = 2$ transmit antennas. This constellation design is based on a *measure preserving mapping* between the unit hypercube and the Grassmannian. This characteristic ensures that any set of uniformly distributed points in the input space (the hypercube) is mapped onto another set of points or codewords uniformly distributed in the output space (the Grassmann manifold). The constellation structure enables on-the-fly symbol generation and low-complexity decoding.

II. System Model

We consider a transmitter with $M = 2$ antennas communicating in a noncoherent MIMO scenario with a receiver equipped with N antennas. We assume a frequency-flat block-fading channel model with coherence time T symbol periods, such that $T \geq 2M$. Hence, the channel matrix $\mathbf{H} \in \mathbb{C}^{M \times N}$ remains constant during each coherence block of T symbols, and changes in the next block to an independent realization. The MIMO channel $\mathbf{H}$ is unknown to both the transmitter and the receiver and assumed to have a Rayleigh fading distribution with entries distributed according to a complex Gaussian distribution with zero mean and unit variance ($h_{ij} \sim \mathcal{CN}(0, 1)$). Within a coherence block, the transmitter sends a unitary

This work was supported by Huawei Technologies Sweden, under the project GRASSCOM. The work of D. Cuevas was also partly supported under grant FPU20/03563 funded by MIU, Spain. The work of Carlos Beltrán was also partly supported under grant PID2020-113887GB-I00 funded by MCIN/ AEI /10.13039/501100011033. The work of I. Santamaria was also partly supported under grant PID2022-137099NB-C43 (MADDIE) funded by MICIU/AEI /10.13039/501100011033 and FEDER, UE.

matrix $\mathbf{X} \in \mathbb{C}^{T\times M}$, $\mathbf{X}^H\mathbf{X} = \mathbf{I}_M$, that is an orthonormal basis for the linear subspace spanned by the columns of $\mathbf{X}$ within $\mathbb{C}^T$. The signal at the receiver $\mathbf{Y} \in \mathbb{C}^{T\times N}$ is[1]

$$\mathbf{Y} = \mathbf{X}\mathbf{H} + \sqrt{\frac{M}{T\rho}}\mathbf{N}\,, \tag{1}$$

where $\mathbf{N} \in \mathbb{C}^{T\times N}$ represents the additive Gaussian noise, with entries modeled as $w_{ij} \sim \mathcal{CN}(0, 1)$, and ρ represents the signal-to-noise-ratio (SNR).

For unitary constellations, the optimal Maximum Likelihood (ML) detector that minimizes the probability of error, assuming equiprobable codewords, is given by

$$\hat{\mathbf{X}} = \arg\max_{\mathbf{X}\in\mathcal{C}} \operatorname{tr}\left(\mathbf{Y}^H\mathbf{P}_{\mathbf{X}}\mathbf{Y}\right)\,, \tag{2}$$

where $\mathcal{C} = \{\mathbf{X}_1, \dots, \mathbf{X}_K\}$ represents the codebook of K codewords and $\mathbf{P}_{\mathbf{X}} = \mathbf{X}\mathbf{X}^H$ is the orthogonal projection matrix onto the column space of $\mathbf{X}$. Each codeword carries $\log_2(K)$ bits of information.

III. Multi-Antenna Grass-Lattice Constellation

A. Overview

The Grass-Lattice constellation is based on a measure preserving mapping from the unit hypercube (product of the interval $(0, 1)$ with itself $2M(T-M)$ times) to the Grassmann manifold, which is the space of M-dimensional subspaces in $\mathbb{C}^T$ denoted as $\mathbb{G}(M, \mathbb{C}^T)$

$$\vartheta : \mathcal{I} = \underbrace{(0, 1) \times \cdots \times (0, 1)}_{2M(T-M)\text{ times}} \to \mathbb{G}\left(M, \mathbb{C}^T\right)\,.$$

It is important to note that $M(T - M)$ is the complex dimension of $\mathbb{G}(M, \mathbb{C}^T)$. The mapping ϑ is composed of three consecutive mappings $\vartheta = \vartheta_3 \circ \vartheta_2 \circ \vartheta_1$:

1) Mapping ϑ_1: from i.i.d. points uniformly distributed in the unit hypercube to i.i.d. points normally distributed in $\mathbb{C}^{(T-M)M}$.
2) Mapping ϑ_2: from i.i.d. points normally distributed in $\mathbb{C}^{(T-M)M}$ to i.i.d. points uniformly distributed in the operator norm unit ball $\mathbb{B}_{\mathbb{C}^{(T-M)\times M},op}(0, 1) = \{\mathbf{W} \in \mathbb{C}^{(T-M)\times M}, \|\mathbf{W}\|_{op} < 1\}$. Here $\|\mathbf{W}\|_{op}$ denotes the operator norm, which is the largest singular value of matrix $\mathbf{W}$.
3) Mapping ϑ_3: from i.i.d. points uniformly distributed in $\mathbb{B}_{\mathbb{C}^{(T-M)\times M},op}(0, 1)$ to i.i.d. points uniformly distributed in $\mathbb{G}(M, \mathbb{C}^T)$.

The composition $\vartheta = \vartheta_3 \circ \vartheta_2 \circ \vartheta_1$ is a measure-preserving mapping that maps points uniformly distributed in $\mathcal{I}$ to points uniformly distributed in $\mathbb{G}(M, \mathbb{C}^T)$. As it was proved in [22], it is possible to find mappings ϑ_1 and ϑ_3 for $M \geq 1$. However, mapping ϑ_2 must be designed specifically for each value of M. We succeeded in doing so for $M = 1$ in [21], [22] and here we derive mapping ϑ_2 for $M = 2$, which will be explained in depth in Section III-B.

Let us first define the $(T - 2) \times 2$ complex matrix, which will be the input to mapping ϑ_1:

$$\mathbf{G} = \begin{pmatrix}\mathbf{a} & \mathbf{b}\end{pmatrix}\,, \tag{3}$$

where $\mathbf{a}$ and $\mathbf{b}$ are column vectors of size $T - 2$ with entries $a_k, b_k \in \mathbb{C}$ and $\Re(a_k), \Re(b_k), \Im(a_k), \Im(b_k) \in (0, 1)$. As we did in [22] for $M = 1$, the real and imaginary components of a_k and b_k will be equispaced points on $[\alpha, 1-\alpha]$, where α is the so-called lattice size.

Now we can define the $(T-2)\times 2$ normal matrix with i.i.d. $\mathcal{CN}(0, 1)$ entries obtained through mapping ϑ_1 as

$$\mathbf{Z} = \begin{pmatrix}\mathbf{r} & \mathbf{s}\end{pmatrix}\,, \tag{4}$$

where the entries of $\mathbf{r}$ are obtained as $r_k = F^{-1}(\Re(a_k)) + jF^{-1}(\Im(a_k))$ and the entries of $\mathbf{s}$ are obtained as $s_k = F^{-1}(\Re(b_k)) + jF^{-1}(\Im(b_k))$, where $F(\cdot)$ is the cdf of a real normal random variable $\mathcal{N}(0, 1/2)$ and j denotes the imaginary unit. This matrix $\mathbf{Z}$ will be the input of mapping ϑ_2.

B. Mapping ϑ_2 for $M = 2$

In this section we describe the mapping ϑ_2, which maps i.i.d. $(T - 2) \times 2$ normal matrices $\mathbf{Z}$ to $(T - 2) \times 2$ uniformly distributed matrices $\mathbf{W}$ in the operator norm unit ball

$$\mathbb{B}_{\mathbb{C}^{2(T-2)},op}(0, 1) = \{\mathbf{W} \in \mathbb{C}^{2(T-2)}, \|\mathbf{W}\|_{op} < 1\}\,.$$

The first step of mapping ϑ_2 is to construct

$$\mathbf{u} = \frac{\mathbf{r}^{\mathrm{H}}\mathbf{s}}{\|\mathbf{r}\|^2}\mathbf{r}\,, \quad \bar{\mathbf{s}} = \mathbf{s} - \mathbf{u}\,, \tag{5}$$

where $\mathbf{u}$ is the projection of $\mathbf{s}$ onto the span of $\mathbf{r}$ and $\bar{\mathbf{s}}$ is the orthogonal component of $\mathbf{s}$ to $\mathbf{r}$. Note that the entries of $\bar{\mathbf{s}}$ and $\mathbf{u}$ are i.i.d. complex normal $\mathcal{CN}(0, 1)$ distributed.

Then, we construct

$$\mathbf{p} = \mathbf{r}h_{T-2}(\|\mathbf{r}\|)\,, \quad \bar{\mathbf{q}} = \bar{\mathbf{s}}h_{T-3}(\|\bar{\mathbf{s}}\|)\,, \tag{6}$$

where $h_{T-2}(\cdot)$ and $h_{T-3}(\cdot)$ are transformations such that $\mathbf{p} \in \mathbb{C}^{T-2}$ has density $\Gamma(T)(1 - \|\cdot\|^2)/\pi^{T-2}$ in the ball $B_{\mathbb{C}^{T-2}}(0, 1)$ and $\bar{\mathbf{q}} \in \mathbb{C}^{T-2}$ has constant density $\Gamma(T-1)(1 - \|\cdot\|^2)/\pi^{T-3}$ in the same ball $B_{\mathbb{C}^{T-2}}(0, 1)$. These functions are defined in Lemma 1 in the Appendix.

Now, we generate

$$\mathbf{v} = \mathbf{u}f_1(\|\mathbf{u}\|)\sqrt{(1 - \|\mathbf{p}\|^2)(1 - \|\bar{\mathbf{q}}\|^2)} \in \mathbb{C}^{T-2}\,, \tag{7}$$

so that $\mathbf{v}$ is uniformly distributed in the disk of radius $\sqrt{(1 - \|\mathbf{p}\|^2)(1 - \|\bar{\mathbf{q}}\|^2)}$ in the space $Span(\mathbf{r})$. Here $f_1(\cdot)$ is given by

$$f_1(\|\mathbf{u}\|) = \frac{1}{\|\mathbf{u}\|}\left(1 - e^{-\|\mathbf{u}\|^2}\right)^{1/2}\,. \tag{8}$$

Finally, we construct the matrix whose first column is $\mathbf{p}$ and whose second column is $\bar{\mathbf{q}} + \mathbf{v}$:

$$\mathbf{W} = \begin{pmatrix}\mathbf{p} & \bar{\mathbf{q}} + \mathbf{v}\end{pmatrix}\,. \tag{9}$$

[1]Here we are adopting the signal model that is commonly used in the noncoherent communications literature, which is equivalent to $\mathbf{Y} = \mathbf{H}\mathbf{X} + \sqrt{M/(T\rho)}\,\mathbf{N}$ when transmitting information over the row space of $\mathbf{X}$.

With this, $\mathbf{W}$ is uniformly distributed in the set of matrices of operator norm at most 1.

IV. Encoding and Decoding

In this section, we describe the whole encoding and decoding procedures of the proposed Grass-Lattice constellation for $M=2$ transmit antennas.

A. Encoder

As we did in [22], we consider 2^B equispaced points on the interval $[\alpha, 1-\alpha]$ for each real and imaginary component of the elements a_k, b_k of matrix $\mathbf{G}$ defined in (3):

$$\hat{x}_p = \alpha + p\,\frac{1-2\alpha}{2^B-1}, \quad 0 \le p \le 2^B - 1\,, \tag{10}$$

where α is a parameter that can be optimized for performance. The uniformly distributed points on the unit cube are chosen randomly from the regular lattice defined by (10). The procedure for computing the codeword to be transmitted $\mathbf{X}$ for an input $a_1, b_1, \ldots, a_{T-2}, b_{T-2}$ is the following:

1) Construct $\mathbf{Z} = \begin{pmatrix}\mathbf{r} & \mathbf{s}\end{pmatrix}$ where $\mathbf{r}$ and $\mathbf{s}$ are vectors of dimension $T-2$ with entries $r_k = F^{-1}(\Re(a_k)) + jF^{-1}(\Im(a_k))$ and $s_k = F^{-1}(\Re(b_k)) + jF^{-1}(\Re(b_k))$, where $F(x)$ is the cdf of a $\mathcal{N}(0, 1/2)$.
2) Compute $\mathbf{u}$ and $\bar{\mathbf{s}}$ as in (5).
3) Construct vectors $\mathbf{p}$ and $\bar{\mathbf{q}}$ as in (6), where $h_n(\cdot)$ is the function defined in Lemma 1 in the Appendix.
4) Generate $\mathbf{v}$ as in (7).
5) Construct the matrix $\mathbf{W}$ as in (9).
6) Output

$$\mathbf{X} = \begin{pmatrix} \left(\mathbf{I}_2 - \mathbf{W}^{\mathrm{H}}\mathbf{W}\right)^{1/2} \\ \mathbf{W} \end{pmatrix}, \tag{11}$$

where $\mathbf{I}_2$ denotes the 2×2 identity matrix.

Notice here that step 1 corresponds to mapping ϑ_1, steps 2-5 to mapping ϑ_2 and step 6 to ϑ_3. The cardinality of the structured Grassmannian constellation is $|\mathcal{C}| = 2^{4B(T-2)}$, and the spectral efficiency is $\eta = \frac{4B(T-2)}{T} = 4B\left(1-\frac{2}{T}\right)$ b/s/Hz.

B. Decoder

The inverse mapping $\vartheta^{-1} : \mathbb{G}(2, \mathbb{C}^T) \to (0,1)^{4(T-2)}$ is obtained by inverting each of the steps of the encoder presented in the previous section. The steps performed by the Grass-Lattice decoder are the following:

1) *Denoising step*: compute the left singular vectors $\mathbf{c}_1$, $\mathbf{c}_2$ corresponding to the two largest singular values of $\mathbf{Y}$ and construct the matrix $\mathbf{C} = \begin{pmatrix}\mathbf{c}_1 & \mathbf{c}_2\end{pmatrix}$.
2) *Invert mapping* ϑ_3: given the matrix $\mathbf{C} = \binom{\mathbf{C}_1}{\mathbf{C}_2}$ representing an element of $\mathbb{G}(2, \mathbb{C}^T)$, let $\mathbf{C}_1 = \mathbf{QP}$ be the polar decomposition of $\mathbf{C}_1$ and let

$$\hat{\mathbf{W}} = \mathbf{C}_2\mathbf{Q}^{\mathrm{H}}\,. \tag{12}$$

3) *Invert step 5 of encoder*: let $\hat{\mathbf{p}}$ be the first column of $\hat{\mathbf{W}}$, let $\mathbf{t}$ be its second column and define:

$$\hat{\mathbf{v}} = \frac{\hat{\mathbf{p}}^{\mathrm{H}}\mathbf{t}}{\|\hat{\mathbf{p}}\|^2}\hat{\mathbf{p}}\,, \quad \hat{\bar{\mathbf{q}}} = \mathbf{t} - \hat{\mathbf{v}}\,. \tag{13}$$

4) *Invert step 4 of encoder*: solve for u in

$$\|\hat{\mathbf{v}}\| = u f_1(u)\sqrt{(1-\|\hat{\mathbf{p}}\|^2)(1-\|\hat{\bar{\mathbf{q}}}\|^2)}\,, \tag{14}$$

and let $\hat{\mathbf{u}} = u\hat{\mathbf{v}}/\|\hat{\mathbf{v}}\|$.
5) *Invert step 3 of encoder*: solve for m and n in

$$\|\hat{\mathbf{p}}\| = m h_{T-2}(m)\,, \quad \|\hat{\bar{\mathbf{q}}}\| = n h_{T-3}(n)\,, \tag{15}$$

and let $\hat{\mathbf{r}} = m\hat{\mathbf{p}}/\|\hat{\mathbf{p}}\|$ and $\hat{\bar{\mathbf{s}}} = n\hat{\bar{\mathbf{q}}}/\|\hat{\bar{\mathbf{q}}}\|$.
6) *Invert step 2 of encoder*: construct

$$\mathbf{s} = \bar{\mathbf{s}} + \mathbf{u}\,. \tag{16}$$

7) *Invert mapping* ϑ_1: compute

$$\hat{a}_k = F(\Re(r_k)) + jF(\Im(r_k))\,, \tag{17}$$

$$\hat{b}_k = F(\Re(s_k)) + jF(\Im(s_k))\,, \tag{18}$$

where $F(x)$ is the cdf of a $\mathcal{N}(0, 1/2)$.
8) Finally, $a_k = \lfloor \hat{a}_k \rceil$ and $b_k = \lfloor \hat{b}_k \rceil$, where $\lfloor x \rceil$ denotes the nearest point to x in the lattice.

TABLE I
Optimal values of the lattice size α for different pairs (T, B).

	$\mathbf{B=1}$	$\mathbf{B=2}$	$\mathbf{B=3}$
$\mathbf{T=4}$	0.22	0.15	0.11
$\mathbf{T=5}$	0.21	0.15	0.13
$\mathbf{T=6}$	0.24	0.18	0.14
$\mathbf{T=7}$	0.23	0.17	0.12
$\mathbf{T=8}$	0.23	0.16	0.14

V. Performance Evaluation

In this section, we evaluate the performance of the proposed Grass-Lattice constellation for $M=2$ transmit antennas and we compare it to another structured Grassmannian constellation named Exp-Map [17]. This constellation is constructed through a non-linear map, called the exponential map, applied to space-time codes for coherent systems. It also uses a simplified decoding rule instead of the ML detector, which makes the performance comparison fair. We have not analyzed the performance of unstructured constellations due to the extremely high complexity of the ML detector for the considered spectral efficiencies.

We first evaluate the influence of α, which determines the length of the lattice used for each real component, on the bit error rate (BER). The BER curves with regard to α are smooth functions with a unique minimum. This minimum, however, cannot be solved in closed form and must be estimated via Monte Carlo simulations. The optimal values of α, which mainly depend on the coherence time T and the number of bits per real component B, can be precomputed offline and are shown in Table I.

Fig. 1 shows the estimated probability density functions of the chordal distance between codewords for the proposed Grass-Lattice constellation, Exp-Map, and uniform distribution on the Grassmann manifold for a scenario with $T=4$ symbol

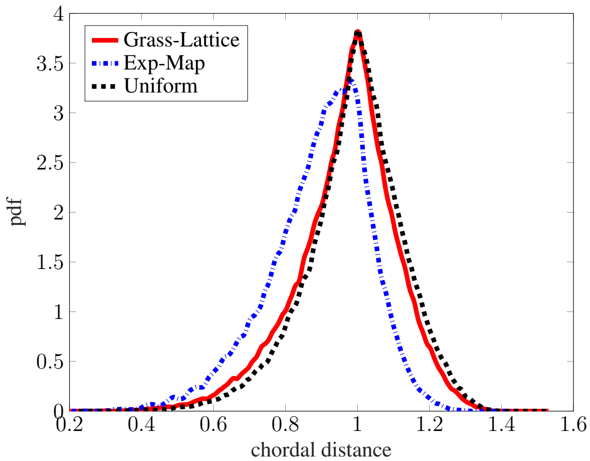

Fig. 1. Estimated probability density functions of chordal distance for Grass-Lattice, Exp-Map and uniform distribution on the Grassmann manifold for $T = 4$ and $\eta = 4$.

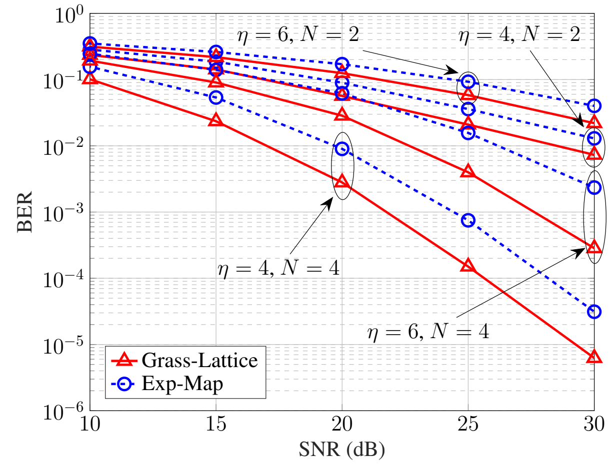

Fig. 2. BER curves of Grass-Lattice and Exp-Map constellations for $T = 4$, $N \in \{2, 4\}$ and $\eta \in \{4, 6\}$.

periods and $\eta = 4$ b/s/Hz. As we can notice, the Grass-Lattice constellation approximates the uniform distribution much better than the Exp-Map constellation, thus achieving a closer distribution to the optimal one in terms of capacity for noncoherent communications under Rayleigh fading channels [3].

In addition to achieving a closer distribution to the optimal one in terms of capacity (uniform distribution), the minimum chordal distance (also called packing efficiency) of the constellation is greater in the case of Grass-Lattice when compared to Exp-Map. This translates into a better BER performance as it is shown in Fig. 2. In this figure, we obtain the BER curves for different scenarios with $T = 4$ symbol periods, $N \in \{2, 4\}$ receive antennas, and $\eta \in \{4, 6\}$ b/s/Hz. We can see that in all cases Grass-Lattice constellations offer superior performance than Exp-Map, with the gap being especially relevant (almost one order of magnitude) when the spectral efficiency is increased.

VI. Conclusions

We have proposed a new Grassmannian constellation for noncoherent communications in MIMO channels with two transmit antennas based on a measure preserving mapping from the unit hypercube to the Grassmann manifold. Thanks to its structure, the encoding and decoding steps can be performed on the fly with no need to store the whole constellation. Further, it allows for low-complexity and efficient encoding-decoding. Simulation results show that this constellation outperforms other unstructured constellations such as Exp-Map in terms of BER under Rayleigh block fading channels.

Appendix

Lemma 1 *Let* $\mathbf{z} = (z_1, \ldots, z_n)^T$ *be i.i.d. such that* $z_i \sim \mathcal{CN}(0, 1)$. *Moreover, for any* $t \geq 0$ *let* $h_n(t)$ *be the unique solution to*

$$(n+1)(th_n(t))^{2n} - n(th_n(t))^{2n+2} = \frac{1}{\Gamma(n)} \int_0^{t^2} s^{n-1} e^{-s}\, ds\,.$$

Then, the random variable

$$\mathbf{x} = \varphi(\mathbf{z}) = \mathbf{z} h_n(\|\mathbf{z}\|)$$

is distributed in the unit ball $\mathbb{B}(0, 1) \subseteq \mathbb{C}^n$ *with probability density function*

$$\rho(x) = \frac{\Gamma(n+2)}{\pi^n}(1 - \|\mathbf{x}\|^2)\,.$$

Proof. The function h_n is the unique solution of:

$$h(t)^{2n-1}(h(t) + th'(t))(1 - t^2h^2) = \frac{e^{-t^2}}{\Gamma(n+2)}, \quad h(0) = 0\,,$$

which satisfies $th(t) \in [0, 1]$ and it is easy to see that $\varphi : \mathbb{C}^n \to \mathbb{B}(0, 1)$ is a diffeomorphism. The Jacobian of φ is:

$$Jac_\varphi(\mathbf{z}) = h_n(\|\mathbf{z}\|)^{2n-1}(h_n(\|\mathbf{z}\|) + \|\mathbf{z}\|h_n'(\|\mathbf{z}\|)) = \frac{e^{-\|\mathbf{z}\|^2}}{\Gamma(n+2)(1 - \|\mathbf{z}\|^2 h_n(\|\mathbf{z}\|)^2)} = \frac{e^{-\|\mathbf{z}\|^2}}{\Gamma(n+2)(1 - \|\varphi(\mathbf{z})\|^2)}\,.$$

Given any integrable mapping $g : \mathbb{B}(0, 1) \to \mathbb{R}$, the expected value of $g(\mathbf{x})$ when $\mathbf{x}$ follows the distribution of the lemma is:

$$\frac{1}{\pi^n} \int_{\mathbf{z}\in\mathbb{C}^n} g(\varphi(\mathbf{z}))e^{-\|\mathbf{z}\|^2}\, d\mathbf{z} = \frac{\Gamma(n+2)}{\pi^n} \int_{\mathbf{z}\in\mathbb{C}^n} g(\varphi(\mathbf{z}))(1 - \|\varphi(\mathbf{z})\|^2) Jac_\varphi(\mathbf{z})\, d\mathbf{z}\,,$$

which by the change of variables theorem equals

$$\frac{\Gamma(n+2)}{\pi^n} \int_{\mathbf{x}\in\mathbb{B}(0,1)} g(\mathbf{x})(1 - \|\mathbf{x}\|^2)\, d\mathbf{x}\,.$$

This is the expected value of g in $\mathbb{B}(0, 1)$ with respect to the claimed volume density. □

REFERENCES

[1] T. Marzetta and B. Hochwald, "Capacity of a mobile multiple-antenna communication link in Rayleigh flat fading," *IEEE Transactions on Information Theory*, vol. 45, no. 1, pp. 139–157, 1999.

[2] B. Hochwald and T. Marzetta, "Unitary space-time modulation for multiple-antenna communication in Rayleigh flat-fading," *IEEE Transactions on Information Theory*, vol. 46, no. 6, pp. 1962–1973, 2000.

[3] L. Zheng and D. Tse, "Communication on the Grassmann manifold: a geometric approach to the noncoherent multiple-antenna channel," *IEEE Transactions on Information Theory*, vol. 48, no. 2, pp. 359–383, 2002.

[4] J. H. Conway, R. H. Hardin, and N. J. A. Sloane, "Packing lines, planes, etc.: Packings in Grassmannian spaces," *Experimental Mathematics*, vol. 5, no. 2, pp. 139–159, 1996.

[5] W. Zhao, G. Leus, and G. B. Giannakis, "Orthogonal design of unitary constellations for uncoded and trellis-coded noncoherent space-time systems," *IEEE Transactions on Information Theory*, vol. 50, no. 6, pp. 1319–1327, 2004.

[6] I. S. Dhillon, R. W. Heath Jr., T. Strohmer, and J. A. Tropp, "Constructing packings in Grassmannian manifolds via alternating projection," *Experimental Mathematics*, vol. 17, no. 1, pp. 9–35, 2008.

[7] M. Beko, J. Xavier, and V. A. N. Barroso, "Noncoherent communications in multiple-antenna systems: receiver design and codebook construction," *IEEE Transactions on Signal Processing*, vol. 55, no. 12, pp. 5703–5715, 2007.

[8] R. H. Gohary and T. N. Davidson, "Noncoherent MIMO communication: Grassmannian constellations and efficient detection," *IEEE Transactions on Information Theory*, vol. 55, no. 3, pp. 1176–1205, 2009.

[9] D. Cuevas, C. Beltrán, I. Santamaria, V. Tuček, and G. Peters, "A fast algorithm for designing Grassmannian constellations," in *25th International ITG Workshop on Smart Antennas (WSA 2021)*, (EURECOM, France), Nov. 2021.

[10] J. Álvarez-Vizoso, D. Cuevas, C. Beltrán, I. Santamaria, V. Tuček, and G. Peters, "Coherence-based subspace packings for MIMO noncoherent communications," in *30th European Signal Processing Conference (EUSIPCO 2022)*, (Belgrade, Serbia), Aug. 2022.

[11] M. L. McCloud, M. Brehler, and M. Varanasi, "Signal design and convolutional coding for noncoherent space-time communication on the block-Rayleigh-fading channel," *IEEE Transactions on Information Theory*, vol. 48, no. 5, pp. 1186–1194, 2002.

[12] D. Cuevas, J. Álvarez-Vizoso, C. Beltrán, I. Santamaria, V. Tuček, and G. Peters, "Union bound minimization approach for designing Grassmannian constellations," *IEEE Transactions on Communications*, vol. 71, no. 4, pp. 1940–1952, 2023.

[13] B. Hochwald, T. Marzetta, T. J. Richardson, W. Sweldens, and R. Urbanke, "Systematic design of unitary space-time constellations," *IEEE Transactions on Information Theory*, vol. 48, no. 6, pp. 1962–1973, 2000.

[14] M. Soleymani and H. Mahdavifar, "Analog subspace coding: A new approach to coding for non-coherent wireless networks," *IEEE Transactions on Information Theory*, vol. 68, no. 4, pp. 2349–2364, 2022.

[15] B. Hughes, "Differential space-time modulation," *IEEE Transactions on Information Theory*, vol. 46, no. 7, pp. 2567–2578, 2000.

[16] R. Pitaval and O. Tirkkonen, "Grassmannian packings from orbits of projective group representations," in *46th Asilomar Conference on Signals, Systems and Computers (Asilomar 2012)*, (Pacific Grove, CA, USA), pp. 478–482, Nov. 2012.

[17] I. Kammoun, A. M. Cipriano, and J. Belfiore, "Non-coherent codes over the Grassmannian," *IEEE Transactions on Wireless Communications*, vol. 6, no. 10, pp. 3657–3667, 2007.

[18] K. Ngo, A. Decurninge, M. Guillaud, and S. Yang, "Cube-split: A structured Grassmannian constellation for non-coherent SIMO communications," *IEEE Transactions on Wireless Communications*, vol. 19, no. 3, pp. 1948–1964, 2020.

[19] G. Han and J. Rosenthal, "Geometrical and numerical design of structured unitary space-time constellations," *IEEE Transactions on Information Theory*, vol. 52, no. 8, pp. 3722–3735, 2006.

[20] S. Li, J.-K. Zhang, and X. Mu, "Design of optimal noncoherent constellations for SIMO systems," *IEEE Transactions on Communications*, vol. 67, pp. 5706–5720, 2019.

[21] D. Cuevas, J. Álvarez-Vizoso, C. Beltrán, I. Santamaria, V. Tuček, and G. Peters, "A measure preserving mapping for structured Grassmannian constellations in SIMO channels," *IEEE Global Communications Conference (GLOBECOM),* (Rio de Janeiro, Brazil), Dec. 2022.

[22] D. Cuevas, J. Álvarez Vizoso, C. Beltrán, I. Santamaria, V. Tuček, and G. Peters, "Constellations on the sphere with efficient encoding-decoding for noncoherent communications," *IEEE Transactions on Wireless Communications*, vol. 23, no. 3, pp. 1886–1898, 2024.